Thermally-Induced Oscillatory Flow and Heat Transfer in a U-Shaped Minichannel

Wei Shao[1] and Yuwen Zhang[2]
University of Missouri, Columbia, MO 65211

Thermally-induced oscillatory flow and heat transfer in a U-shaped minichannel – a building block of an Oscillating Heat Pipe (OHP) – is modeled by analyzing evaporation and condensation in the heating and cooling sections, effect of axial variation of surface temperature on sensible heat transfer between the liquid slug and the minichannel wall, as well as pressure loss at the bend. The oscillatory flow of the liquid slug is driven by variations of pressures of the vapor plug due to evaporation and condensation. The sensible heat transfer coefficient between the liquid slug and the minichannel wall are obtained by analytical solution for laminar liquid flow and by empirical correlations for turbulent liquid flow. The effects of the initial temperature and pressure loss at bend on the heat transfer performance are thoroughly investigated.

Nomenclature

A	=	area, m^2
c_p	=	specific heat at constant pressure, J/kg-K
c_v	=	specific heat at constant volume, J/kg-K
d	=	diameter of the miniature channel, m
G_n	=	constant
h_{lv}	=	Latent heat of vaporization, J/kg
h_e	=	evaporation heat transfer coefficient, W/m^2-K
h_c	=	condensation heat transfer coefficient, W/m^2-K
k	=	thermal conductivity, W/m-K
K	=	loss coefficient
L	=	length, m
m	=	mass of vapor plugs, kg
$\dot{m}$	=	mass flow rate, kg/s
Nu	=	Nusselt number
p	=	vapor pressure, Pa
R	=	gas constant, J/kg-K
t	=	time, s
T	=	temperature, K
v_p	=	velocity of the liquid plug, m/s
x_p	=	displacement of the liquid plug, m
x^+	=	dimensionless coordinates on the liquid plug
$Q_{p,eva}$	=	evaporation heat transfer, W
$Q_{p,con}$	=	condensation heat transfer, W
$Q_{in,p,l}$	=	sensible heat transfer into the liquid plug, W
$Q_{out,p,l}$	=	sensible heat transfer out of the liquid plug, W

Greek symbols

α	=	thermal diffusivity, m^2/s
γ	=	ratio of specific heats
ν	=	kinematic viscosity, m^2/s

[1] Graduate Research Assistant, Department of Mechanical and Aerospace Engineering.
[2] Professor, Department of Mechanical and Aerospace Engineering, Associate Fellow AIAA.

ρ = density, kg/m^3
τ = shear stress, N/m^2
λ_n = eigenvalue
ξ = dimensionless coordinate where wall temperature varies
Δ = difference

Subscripts

0 = initial condition
c = condenser
e = evaporator
l = liquid
m = mean

I. Introduction

OSCILLATING Heat Pipe (OHP) is a very promising heat transfer device that can be utilized to transfer a large amount of heat from heating to cooling sections. The research and development of the OHP, like conventional heat pipes, has speeded up since 1990s due to increasing demands for faster and smaller microelectronic systems[1]. As the chips in computer and power electronics become smaller and more densely packed, more efficient cooling systems are needed. For instance, the new design of the computer chip by Intel will produce localized heat flux over 100 W/cm^2 with the total power exceeding 300 W. In addition to the limitation on the maximum temperature, electronic components also have constraints on the level of temperature uniformity[2]. OHP is a very promising technology for achieving high local heat-removal rates and uniform temperatures on the computer chips.

Typically, an OHP consists of a plain meandering long tube of capillary dimensions with many U-turns and joined end to end and the evaporator and condenser sections are located at these turns. Compared with the traditional heat pipes, the unique feature of OHP is that the vapor and liquid flow in the same direction, and therefore there is no friction between the liquid and vapor phases. The inner diameter of an OHP should be sufficiently small to ensure the formation of liquid slugs by capillary effect. If the diameter is too large, the liquid and vapor phases tend to stratify[3]. Due to the oscillation of the working fluid in the axial direction of the tube, heat is transported from the evaporator section to the condenser section by the liquid slugs via sensible heat, which is dominant when the flow pattern in the OHP is slug flow[4]. At the cold state, the liquid slugs in the OHP are in their equilibrium positions. If triggered by the starting pulse, the liquid slugs depart from their equilibrium positions and oscillation is initiated. The heat input, acting as the driving force, increases the pressure of the vapor plug in the evaporator section. Meanwhile, another factor to cause liquid slug moving is that condensation that takes place in the condenser section that results in decrease of the vapor pressure. The pressure difference can also change its sign as the oscillation of the liquid causes the vapor plugs that was originally in the evaporator (condenser) section moves to the condenser (evaporator) section. This process is repeated and the oscillation of the liquid plug can be sustained by the thermally induced pressure difference inside the OHP and no external mechanical power is required.

In the last decade, extensive experimental and theoretical works have been conducted to understand the mechanism of the OHP. Khandekar et al.[5, 6], Rittidech et al.[7], and Tong et al. [8] studied the effects of many parameters – such as internal diameter, number of turns, working fluid and inclination angle – on the flow and heat transfer. The results demonstrated that OHP with many turns were able to perform satisfactorily independent of inclination angle while heat flux decreases as the number of turns increases. It was proposed that some optimum number of turns that would achieve maximum heat flux might exist. Dobson and Harms[9] developed a simple mathematical model to study the behavior of an OHP with an open-end. Zhang et al.[10] and Shafii et al.[11, 12] concluded that overall heat transfer is dominated by sensible heat transfer, and the frequency and amplitude are not affected by surface tension. Groll and Khandekar[13] showed that for ethanol the ratio of sensible enthalpy is greater than 98% for the range of charge ratios in which OHPs operate and indicated that a low surface tension was desirable because it reduces the pressure drop necessary to drive the flow. Liang and Ma[14] presented a mathematical model describing the oscillation characteristics of slug flow in a capillary tube. It was demonstrated that the internal diameter, vapor plug size, and unit cell numbers determine the oscillation and capillary force. Initial pressure and distribution of the working fluid significantly affects the frequency and amplitude of oscillating motion in the capillary tube. Zhang and Faghri[15] investigated liquid-vapor pulsating flow in OHP with arbitrary number of turns. The results showed that for an OHP with fewer than six turns the amplitude and frequency of oscillation are independent of the number of turns. Ma et al.[16] developed a mathematical model predicting the fluid motion and temperature drop in an OHP. The numerical results indicate that the oscillating motions occurring in the OHP

significantly enhances the heat transfer in the OHP. Experimental results indicated that there exists an onset temperature difference for the excitation of oscillating motions in an OHP.

While these investigations have provided an insight into the mechanisms of oscillating motions occurring in the OHP, there were some oversimplifications in the existing theoretical model for OHP. For example, none of the existing models considered the effect of axial variation of the surface temperature, initial temperature, and pressure loss in the bend on the performance of the OHP. Thermal analysis of oscillating flow and heat transfer in a U-shaped minichannel will be presented in this paper. The effects of initial temperature, axial variation of the surface temperature, pressure loss in bend on the performance of oscillating heat pipe will be thoroughly investigated.

II. Theoretical Model

The physical model is a vertically placed U-shaped minichannel (see Fig. 1(a)) with its two ends sealed. The U-shaped minichannel is treated as a straight tube (see Figure 1(b)) with the pressure loss at the bend considered. The length of each heating section, which is located at the two ends of the pipe, is L_e and its wall temperature is T_e. The cooling section with wall temperature is T_c is located between two evaporation sections and its length is L_c. The length of the liquid slug is L_p and x_p is used to represent the displacement of the liquid slug. When the liquid slug is exactly in the middle of the U-shaped miniature channel, x_p is zero. When the liquid slug shifts to the right side, x_p is positive; when it moves to the left side x_p is negative.

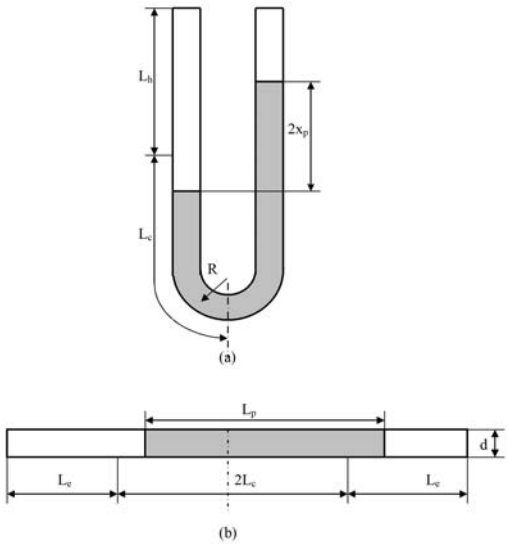

Figure 1 Physical Model

If the initial value of displacement x_{p0} is positive, part of the vapor plug in the left-side is in contact with the condenser section, and condensation in the left part will cause the pressure of the left vapor plug p_{v1} to decrease. The pressure difference between the two vapor plugs causes the liquid slug moving to the left direction. Evaporation from the thin liquid film left behind on the right part of the channel cause the pressure of the right vapor plug p_{v2} to increase and the pressure difference between the two ends of the liquid slug further increases. When the displacement x_p becomes zero, there is neither evaporation nor condensation in two vapor plugs, but the liquid slug keeps moving due to its inertia. When the liquid moves to the left side ($x_p < 0$), the pressure difference changes its sign. The oscillation of the liquid slug can be sustained by alternative evaporation and condensation in the two vapor plugs.

The following assumptions are made in order to model heat transfer and fluid flow in the heat pipe:

(1) The liquid is incompressible and the vapor plugs are assumed to behave as ideal gases.
(2) Evaporative and condensation heat transfer coefficients are assumed to be constants.
(3) Heat conduction in the liquid slug is assumed to be one-dimensional in the axial direction and exchange of heat between the liquid and wall is considered by a convective heat transfer coefficient.
(4) The U-shaped minichannel is assumed to be a straight pipe and the effect of pressure loss in the bend is considered using an empirical correlation.

A. Governing Equations

The momentum equation for the liquid slug is:

$$AL_p\rho_l \frac{d^2x_p}{dt^2} = [(p_{v1} - p_{v2}) - \Delta p_b]A - 2\rho_l g A x_p - \pi d L_p \tau_p \tag{1}$$

where $A = \pi d^2 / 4$ is cross-sectional area and $\tau_p = c_l \rho v^2 / 2$ is the shear stress

$$c_l = \begin{cases} 16/\mathrm{Re} & \mathrm{Re} \le 2200 \\ 0.078\,\mathrm{Re}^{-0.2} & \mathrm{Re} > 2200 \end{cases} \tag{2}$$

and Δp_b is the pressure loss at the bend[17]:

$$\Delta p_b = \begin{cases} K\rho_l \dfrac{v_p^{\,2}}{2} & v_p > 0 \\ -K\rho_l \dfrac{v_p^{\,2}}{2} & v_p < 0 \end{cases} \tag{3}$$

where K is the pressure loss coefficient. The effect of gravity on the motion of the liquid slug has been included in the momentum equation.

The energy equations of the two vapor plugs are:

$$\frac{d(m_{v1}c_vT_{v1})}{dt} = c_pT_{v1}\frac{dm_{v1}}{dt} - p_{v1}\frac{\pi}{4}d^2\frac{dx_p}{dt} \tag{4}$$

$$\frac{d(m_{v2}c_vT_{v2})}{dt} = c_pT_{v2}\frac{dm_{v2}}{dt} - p_{v2}\frac{\pi}{4}d^2\frac{dx_p}{dt} \tag{5}$$

The vapor plugs behave as an ideal gas, i.e.,

$$p_{v1}(L_e + x_p)\frac{\pi}{4}d^2 = m_{v1}RT_{v1} \tag{6}$$

$$p_{v2}(L_e - x_p)\frac{\pi}{4}d^2 = m_{v2}RT_{v2} \tag{7}$$

Differentiating eqs. (6) and (7) with respect to time yields:

$$\frac{\pi}{4}d^2\frac{dp_{v1}}{dt}(L_e + x_p) + p_{v1}\frac{\pi}{4}d^2\frac{dx_p}{dt} = m_{v1}R\frac{dT_{v1}}{dt} + RT_{v1}\frac{dm_{v1}}{dt} \tag{8}$$

$$\frac{\pi}{4}d^2\frac{dp_{v2}}{dt}(L_e - x_p) + p_{v2}\frac{\pi}{4}d^2\frac{dx_p}{dt} = m_{v2}R\frac{dT_2}{dt} + RT_{v2}\frac{dm_{v2}}{dt} \tag{9}$$

which can be substituted into eqs. (8) and (9) to obtain:

$$\frac{1}{m_{v1}}\frac{dm_{v1}}{dt} = \frac{1}{\gamma}\frac{1}{p_{v1}}\frac{dp_{v1}}{dt} + \frac{1}{L_e + x_p}\frac{dx_p}{dt} \tag{10}$$

$$\frac{1}{m_{v2}}\frac{dm_{v2}}{dt} = \frac{1}{\gamma}\frac{1}{p_{v2}}\frac{dp_{v2}}{dt} + \frac{1}{L_e + x_p}\frac{dx_p}{dt} \tag{11}$$

where $\gamma = c_p / c_v$ is the ratio of specific heats of the vapor.

Integrating eqs. (10) and (11), the masses of vapor plugs are obtained as:

$$m_{v1} = C_1 p_{v1}^{\frac{1}{\gamma}}(L_e + x_p) \tag{12}$$

$$m_{v2} = C_2 p_{v2}^{\frac{1}{\gamma}}(L_e - x_p) \tag{13}$$

where C_1 and C_2 are integral constants. Since the structure of the U-shaped channel is symmetric, the two integral constants are the same, i.e., $C_1 = C_2 = C$. Substituting eqs. (12) and (13) into eqs. (6) and (7), one obtains the temperatures of both vapor plugs:

$$T_{v1} = \frac{\pi d^2}{4CR}p_{v1}^{\frac{(\gamma-1)}{\gamma}} \tag{14}$$

$$T_{v2} = \frac{\pi d^2}{4CR}p_{v2}^{\frac{(\gamma-1)}{\gamma}} \tag{15}$$

The integral constant can be determined by choosing a reference state that the displacement of liquid slug is x_{p0} and pressures and temperatures of both vapor plugs are T_0, p_0, respectively. It follows from eqs. (14) and (15) that

$$C_1 = C_2 = C = \frac{\pi d^2}{4RT_0}p_0^{\frac{(\gamma-1)}{\gamma}} \tag{16}$$

Substituting eq. (16) into eqs. (12) – (15), the masses and temperatures of two vapor plugs become:

$$m_{v1} = \frac{\pi d^2 p_0}{4RT_0}\left(\frac{p_{v1}}{p_0}\right)^{\frac{1}{\gamma}}(L_e + x_p) \tag{17}$$

$$m_{v2} = \frac{\pi d^2 p_0}{4RT_0}\left(\frac{p_{v2}}{p_0}\right)^{\frac{1}{\gamma}}(L_e - x_p) \tag{18}$$

$$T_{v1} = T_0\left(\frac{p_{v1}}{p_0}\right)^{\frac{(\gamma-1)}{\gamma}} \tag{19}$$

$$T_{v2} = T_0\left(\frac{p_{v2}}{p_0}\right)^{\frac{(\gamma-1)}{\gamma}} \tag{20}$$

The effects of evaporation and condensation on variation of the masses of the vapor plugs can be calculated as following,

$$\frac{dm_{v1}}{dt} = \begin{cases} -h_c \pi d x_p \left(T_{v1} - T_c\right)/h_{lv,} & x_p > 0 \\ -h_e \pi d \left(L_e + x_p\right)\left(T_e - T_{v1}\right)/h_{lv,} & x_p < 0 \end{cases} \tag{21}$$

$$\frac{dm_{v2}}{dt} = \begin{cases} h_e \pi d \left(L_e - x_p\right)\left(T_e - T_{v2}\right)/h_{lv,} & x_p > 0 \\ h_c \pi d x_p \left(T_{v2} - T_c\right)/h_{lv,} & x_p < 0 \end{cases} \tag{22}$$

The initial condition of the U-shaped minichannel in this study is chosen to be identical to the reference state of this system, i.e.,

$$x_p = x_{p0,}\ t = 0 \tag{23}$$

$$p_{v1} = p_{v2} = p_0,\ t = 0 \tag{24}$$

$$T_{v1} = T_{v2} = T_0,\ t = 0 \tag{25}$$

$$m_{v1} = \frac{\pi d^2 p_0}{4RT_0}(L_e + x_{p0}) \tag{26}$$

$$m_{v2} = \frac{\pi d^2 p_0}{4RT_0}(L_e - x_{p0}) \tag{27}$$

B. Heat Transfer

Heat transfer in an OHP is defined as the total heat transferred from the heating sections to the cooling sections that consists of two parts: one is the latent heat transfer due to evaporation and condensation of the working fluid, and another part is sensible heat transfer due to heat transfer between the minichannel wall and liquid slugs in the form of single-phase heat transfer.

The evaporation and condensation heat transfer in the left and right vapor plugs is related to the mass flux due to evaporation and condensation:

$$Q_{in,v1} = \dot{m}_{evp,v1} h_{lv} \tag{28}$$

$$Q_{out,v1} = \dot{m}_{con,v1} h_{lv} \tag{29}$$

$$Q_{in,v2} = \dot{m}_{evp,v2} h_{lv} \tag{30}$$

$$Q_{out,v2} = \dot{m}_{con,v2} h_{lv} \tag{31}$$

Since the liquid slug is assumed to be incompressible, the entire liquid slug oscillates with the same velocity v_p. The temperature distribution in the liquid slug can be obtained by solving the energy equation for a liquid slug in a coordinate system that is moving with the liquid slug:

$$\frac{1}{\alpha_l}\frac{dT_l}{dt} = \frac{d^2 T_l}{dx_l^{\,2}} - \frac{h_{lsen}\pi d}{k_l A}\left(T_l - T_w\right) \tag{32}$$

where the thermophysical properties of the liquid slug is based on the mean temperature of the liquid slug. Equation (32) is subject to the following initial and boundary conditions

$$T = T_0,\ t = 0,\ 0 < x_l < L_p \tag{33}$$

$$T = T_{v1},\ x_l = 0 \tag{34}$$

$$T = T_{v2},\ x_l = L_p \tag{35}$$

The wall temperature of the tube can be either T_e or T_c, depending on the displacement of the liquid slug, i.e.,

When $x_p > 0$,

$$T_w = \begin{cases} T_c, & 0 < x_l < L_p - x_p \\ T_e, & L_p - x_p < x_l < L_p \end{cases} \tag{36}$$

When $x_p < 0$,

$$T_w = \begin{cases} T_e, & 0 < x_l < \left|x_p\right| \\ T_c, & \left|x_p\right| < x_l < L_p \end{cases} \tag{37}$$

Since the Reynolds number of the liquid slug varies in a wide range that covers laminar, transition and turbulent flow, the heat transfer coefficient h of the liquid slug varies periodically. For laminar regime, ($\mathrm{Re} < 2200$), the convective heat transfer problem is considered as thermally developing Hagen-Poiseuille flow. With the effect of axial step variation of surface temperature considered, the Nusselt number is obtained using method of superposition[18]:

$$\mathrm{Nu}(x) = \begin{cases} \dfrac{\sum_{n=0}^{\infty} G_n \exp(-\lambda_n^2 x^+)}{2\sum_{n=0}^{\infty}\left(\dfrac{G_n}{\lambda_n^2}\right)\exp(-\lambda_n^2 x^+)}, & 0 < x^+ < \xi \\ \dfrac{\sum_{n=0}^{\infty} G_n \exp(-\lambda_n^2 x^+)\Delta T_{l,\mathrm{I}} + \sum_{n=0}^{\infty} G_n \exp\left[-\lambda_n^2\left(x^+ - \xi\right)\right]\Delta T_{l,\mathrm{II}}}{2\sum_{n=0}^{\infty}\left(\dfrac{G_n}{\lambda_n^2}\right)\exp(-\lambda_n^2 x^+)\Delta T_{l,\mathrm{I}} + 2\sum_{n=0}^{\infty}\left(\dfrac{G_n}{\lambda_n^2}\right)\exp\left[-\lambda_n^2(x^+ - \xi)\right]\Delta T_{l,\mathrm{II}}}, & \xi < x^+ < L_p^+ \end{cases} \tag{38}$$

where $L_p^+ = 2L_p/(d\,\mathrm{Re}\,\mathrm{Pr})$ is dimensionless length of the liquid slug, and the eigenvalues λ_n and the constant G_n can be found in Kays et al.[18]. The parameters and variables used in eq. (38) are different for different displacements and direction of liquid flow (see Table 1). In contrast to the existing models in the literature that assumed constant latent heat transfer coefficient, variation of Nusselt number along the length of the liquid slug is taken into consideration.

Table 1 Parameters and variables for laminar sensible heat transfer, eq. (38)

	x^+	ξ	$\Delta T_{l,\mathrm{I}}$	$\Delta T_{l,\mathrm{II}}$
$x_p > 0, v_p > 0$	$\dfrac{2(x_l/d)}{\mathrm{Re}\,\mathrm{Pr}}$	$\dfrac{2\left(\left(L_p - x_p\right)/d\right)}{\mathrm{Re}\,\mathrm{Pr}}$	$T_c - T_{v1}$	$T_e - T_c$
$x_p > 0, v_p < 0$	$\dfrac{2\left(\left(L_p - x_l\right)/d\right)}{\mathrm{Re}\,\mathrm{Pr}}$	$\dfrac{2\left(x_p/d\right)}{\mathrm{Re}\,\mathrm{Pr}}$	$T_e - T_{v2}$	$T_c - T_e$
$x_p < 0, v_p > 0$	$\dfrac{2(x_l/d)}{\mathrm{Re}\,\mathrm{Pr}}$	$\dfrac{2\left(-x_p/d\right)}{\mathrm{Re}\,\mathrm{Pr}}$	$T_e - T_{v1}$	$T_c - T_e$
$x_p < 0, v_p < 0$	$\dfrac{2\left[\left(L_p - x_l\right)/d\right]}{\mathrm{Re}\,\mathrm{Pr}}$	$\dfrac{2\left[\left(L_p + x_p\right)/d\right]}{\mathrm{Re}\,\mathrm{Pr}}$	$T_c - T_{v2}$	$T_e - T_c$

In the transition and turbulent regions, the following empirical correlations are used [11]:

$$Nu = 0.012(|\mathrm{Re}|^{0.87} - 280)\,\mathrm{Pr}^{0.4}\left(\frac{\mathrm{Pr}_m}{\mathrm{Pr}_w}\right)^{0.11}\left[1+\left(\frac{d}{L_p}\right)^{\frac{2}{3}}\right],\quad 2200 < \mathrm{Re} < 10000 \tag{39}$$

$$Nu = 0.0236|\mathrm{Re}|^{0.8}\,\mathrm{Pr}^{0.43}\left(\frac{\mathrm{Pr}_m}{\mathrm{Pr}_w}\right)^{0.25},\ |\mathrm{Re}| > 10000 \tag{40}$$

The sensible heat transfer into and out from the liquid slug can be obtained by integrating the heat transfer over the length of the liquid slug, i.e.

$$Q_{in,s,l} = \begin{cases} \int_{L_p - x_p}^{L_p} \pi dh(T_e - T_l)dx_l,\ x_p > 0 \\ \int_0^{|x_p|} \pi dh(T_e - T_l)dx_l,\ x_p < 0 \end{cases} \tag{41}$$

$$Q_{out,s,l} = \begin{cases} \int_0^{-x_p} \pi dh(T_l - T_c)dx_l,\ x_p > 0 \\ \int_{|x_p|}^{L_p} \pi dh(T_l - T_c)dx_l,\ x_p < 0 \end{cases} \tag{42}$$

where the sensible heat transfer coefficient can be obtained from $h = Nuk_l / d$.

III Numerical Procedure

The governing equations in the above physical model can be solved numerically. An explicit finite difference scheme is employed to solve the governing equations of the vapor plug and the liquid slug. An implicit scheme with uniform grid[19] is employed to solve transient heat transfer in the liquid slug. The results of each time-step can be obtained by following the numerical procedure outlined below:

1) Assume the temperatures of the two vapor plugs T_{v1} and T_{v2}, and calculate thermal and physical properties of liquid according to T_l
2) Solve for vapor pressures, p_{v1} and p_{v2}, from eqs. (14) and (15).
3) Solve for x_p from eqs. (1) and (2).
4) Obtain the new masses of the two vapor plugs m_{v1} and m_{v2}, by accounting for the change of vapor masses from eqs. (21) and (22).
5) Calculate the pressure of the two vapor plugs, p_{v1} and p_{v2}, from eqs. (14) and (15).
6) Solve for T_{v1} and T_{v2} from eqs. (19) and (20).
7) Compare T_{v1} and T_{v2} obtained in Step 6 with assumed values in step 1. If the differences meet the small tolerance, then go to the step 8; otherwise, the above procedure is repeated until a converged solution is obtained.
8) Obtain heat transfer coefficient through eqs. (38) to (40).
9) Solve for liquid temperature distribution from eq. (32) and calculate Q_s.
10) Use eqs. (28) and (31) to calculate Q_{latent}

After the time-step independent test, it was found that the time-step independent solution of the problem can be obtained when time-step is $\Delta t = 1\times10^{-4}$, which is used in all numerical simulations.

IV Results and Discussion

In order to validate the present model, oscillatory flow in the U-Shaped minichannel with the parameters same as those used by Zhang et al.[10] is simulated first. The pressure loss at bend was neglected and the thermophysical properties of liquid and vapor treated as temperature-independent for this case only. The parameters used in simulation are: $L_e = 0.1m$, $L_c = 0.1m$, $L_p = 0.2m$, $d = 3.34mm$, $T_e = 123.4^\circ C$, $T_c = 20^\circ C$, and $h_e = h_c = 200$ W/m^{2}K . Figure 2 shows the variations of liquid slug displacement, x_p , vapor pressure, p_v , and the vapor temperature, T_v , with time for the present model and those by Zhang et al.[10]. The frequency and amplitude of the displacement of the liquid slug shown in Fig. 2(a) are identical as those of Zhang et al.[10]. The temperature and

pressure of vapor plugs obtained by using the present model agreed very well with those by Zhang et al.[10]. Thus, the variation of Nusselt number in laminar region has very insignificant effect on the oscillatory fluid flow.

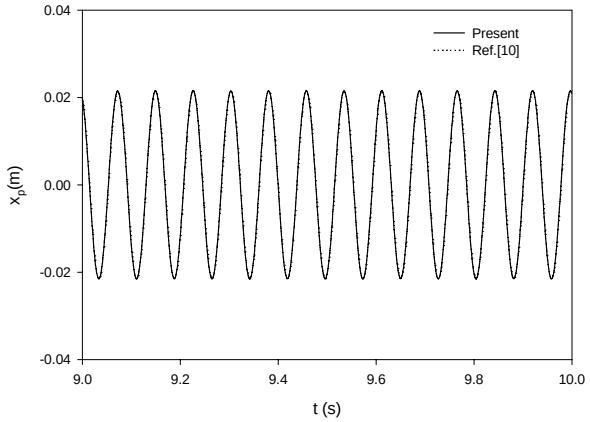

(a) Liquid slug displacement

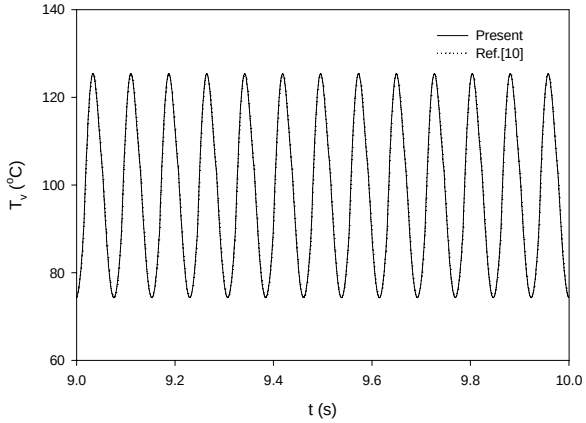

(b) Vapor temperature

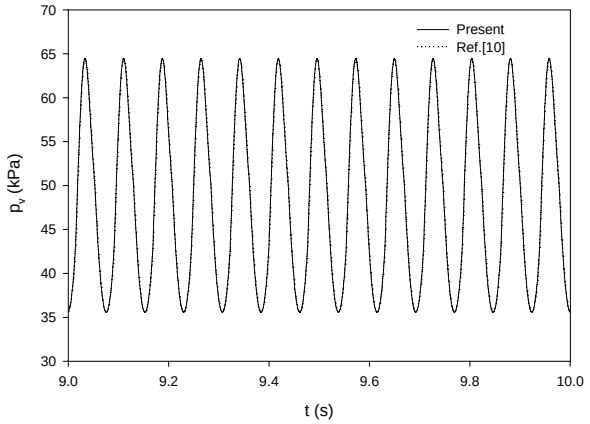

(c) Vapor pressures

Figure 2 Comparison of liquid slug displacement, vapor temperatures and pressures

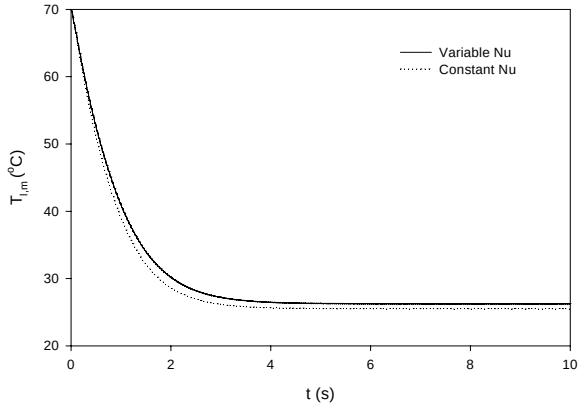

Figure 3 Average mean temperatures of liquid slug

Figure 3 shows the effect of different Nusselt number on the mean temperature of the liquid slug. As the heat transfer coefficient between the liquid slug and the wall is not treated as uniform, the calculation of heat transfer coefficient is more accurate than the method used in the existing works. For the same heating and cooling temperatures, the result from the variable Nusselt number model has a smoother transition from startup to steady oscillating motion. For variable Nu model, the steady-state is reached a little slower than the constant Nu model. The final temperature of the liquid slug for variable Nu model is slightly higher than that for constant Nu model because the heat transfer coefficients for segment I in heating and cooling section are higher under the variable Nu model. The current model includes the effect of thermal entry length on heat transfer and the axial temperature variation for is laminar regime.

Figure 4(a) and (b) show sensible heat transfer into and out from liquid slug for both variable and constant Nu models. After taking the effect of axial variation of surface temperature into account, the sensible heat transferred in and out is almost the same as that of the original model when the flow is turbulent. On the contrary, the sensible heat transfer for the variable Nu model in the laminar region is higher than that for the constant Nu model. The average sensible heat transfer rate is increased from 40.85 for constant Nu model to 42.72W for variable Nu model, which is a 4.5% increase. Thus, the effect of axial variation of surface temperature for laminar regime on convective heat transfer on the overall heat transfer is important.

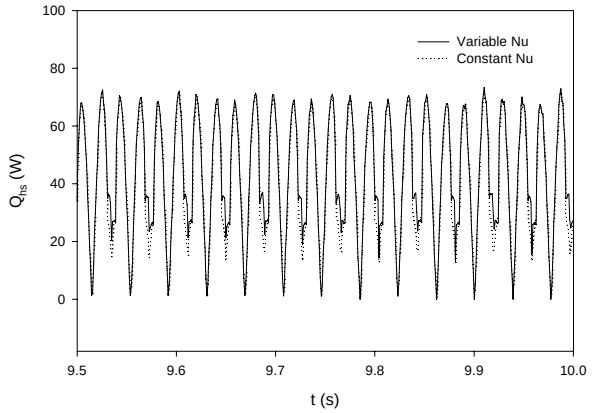

(a) Sensible heat transferred into the liquid slug

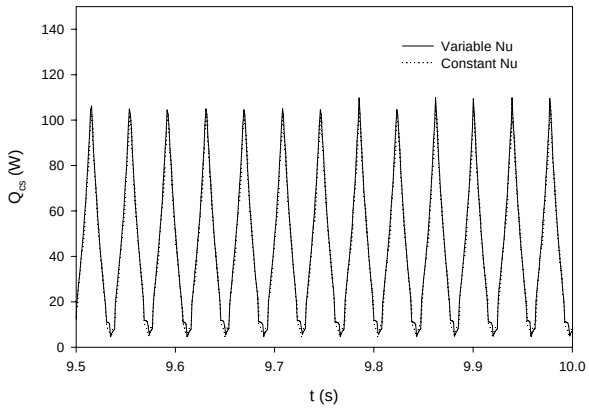

(b) Sensible heat transferred out from the liquid slug

Figure 4 Sensible heat transfer

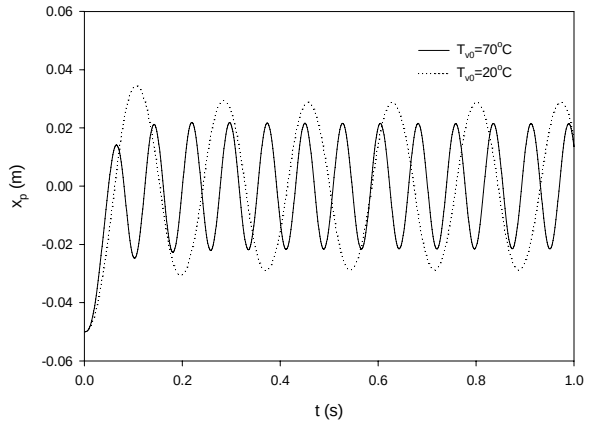

(a) Startup stage

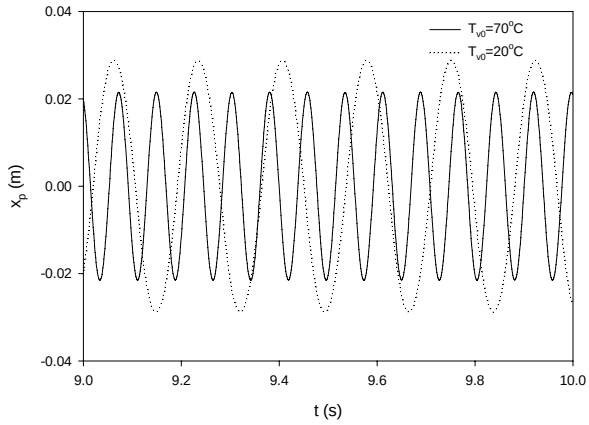

(b) Steady oscillation stage

Figure 5 Displacement of liquid slug for initial temperature

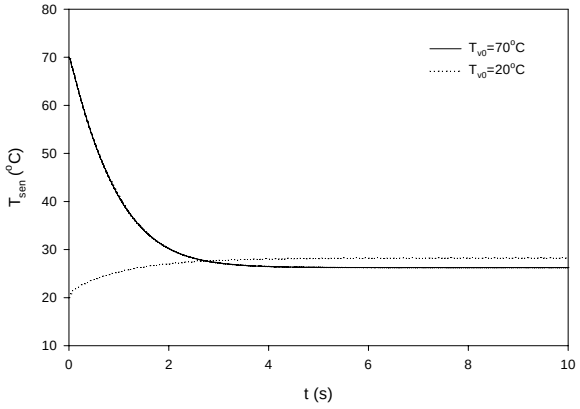

Figure 6 Average mean temperatures of liquid slug

The effect of the initial temperatures on the oscillatory flow and heat transfer in the U-shaped minichannel is then studied and the results are shown in Figs. 5 through 10. Figure 5(a) shows the effect of the initial temperatures of vapor slugs on the displacement of the liquid slugs during the first one second. The decrease of initial temperature has significant effects on the amplitudes and angular frequencies of liquid slug oscillation. The liquid slug exhibited huge fluctuation at the first second and the phase of oscillation also recedes with decreasing temperatures of vapor plugs. Figure 5(b) shows the effect of the initial temperatures on the displacement of liquid slugs after steady oscillation is established. The maximum displacement of the liquid slug oscillation with an initial temperature of $20^{\circ}C$ is 0.0288m, which is larger than 0.0214m for the maximum displacement for the initial temperature of

70 °C. The period of liquid slug oscillation is 0.172 second when the initial temperature is 20 °C, which is much longer than the period of 0.077 second when the initial temperature is 70 °C. As a result, the laminar flow plays more important role with lower initial temperature. Figure 6 shows the transient response of average mean temperature of liquid slug to different initial temperature. The steady oscillation was achieved almost at the same time for both cases. However, the liquid temperature for the initial temperature of 20 °C is a little higher than that for the initial temperature of 70 °C.

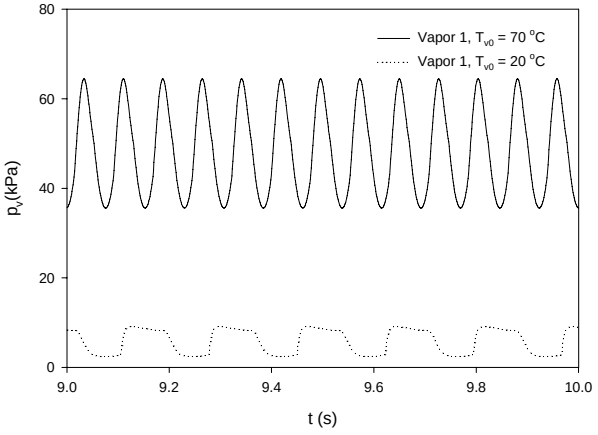

(a) Left vapor plug

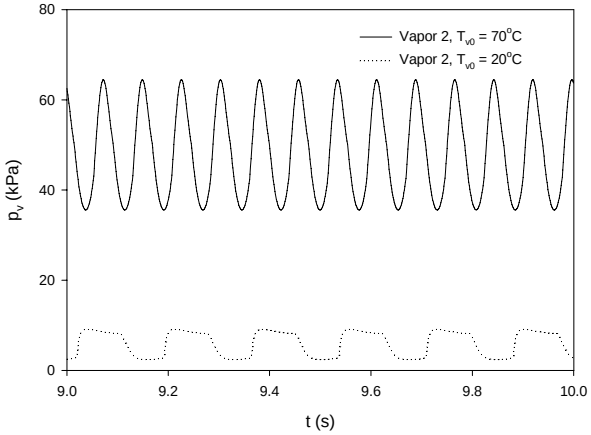

(b) Right vapor plug

Figure 7 Vapor pressures at different initial temperatures

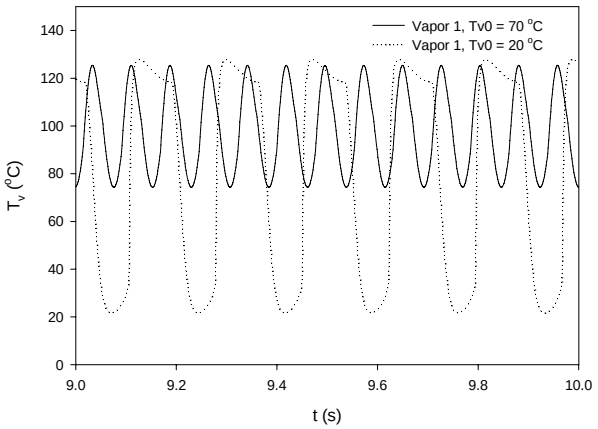

(a) Left vapor plug

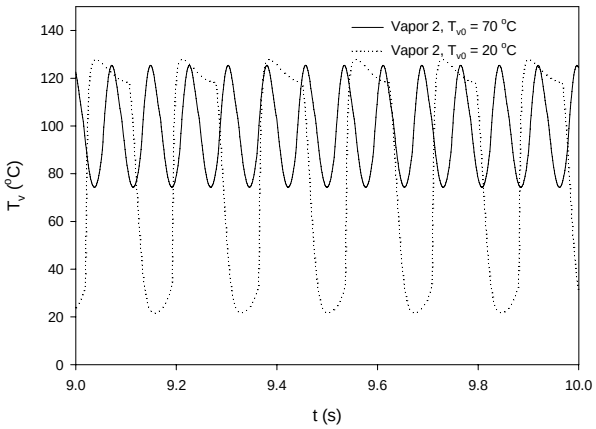

(b) Right vapor plug

Figure 8 Vapor temperatures for different initial temperature

Figure 7 and 8 show the variation of pressures and temperatures for both vapor plugs at different initial temperatures. When the initial temperature is low, the corresponding saturation pressure is low. The saturation pressure corresponding to 20 °C for water is 2336.8 Pa while the saturation pressure for water at 70 °C is 33639Pa. The vapor pressures and temperatures, as shown in Figs. 7 and 8, exhibit similar trends as that of the liquid slug displacement except the oscillating ranges of pressure for different initial temperatures are different. The amplitude of pressure for initial temperature of 20 °C is much smaller than that for initial temperature of 70 °C. With the same heating and cooling temperatures, the lowest temperatures of the vapor plugs can reach for both different initial temperatures are very different. On the contrary, the highest temperatures of vapor plugs for different initial temperatures are almost the same (see Fig. 8).

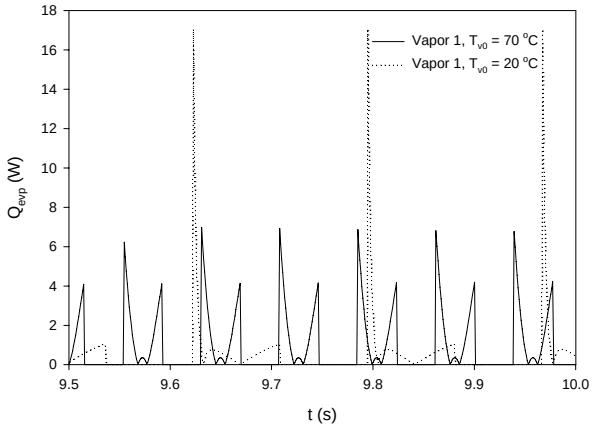

(a) Evaporation

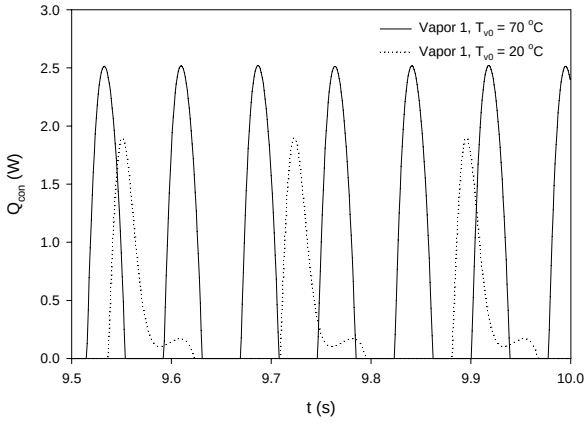

(b) Condensation

Figure 9 Evaporation and condensation of the left vapor plug for different initial temperature

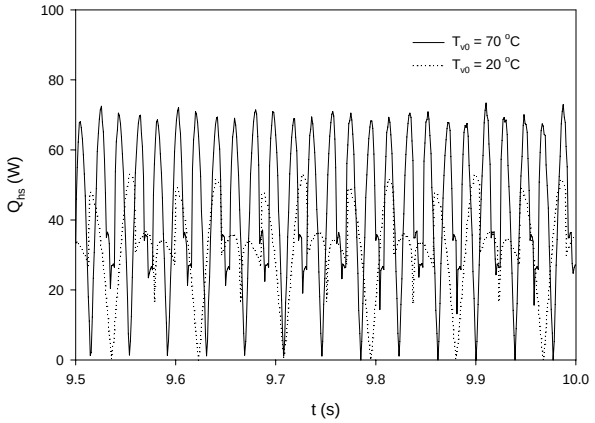

Sensible heat transferred into the liquid slug

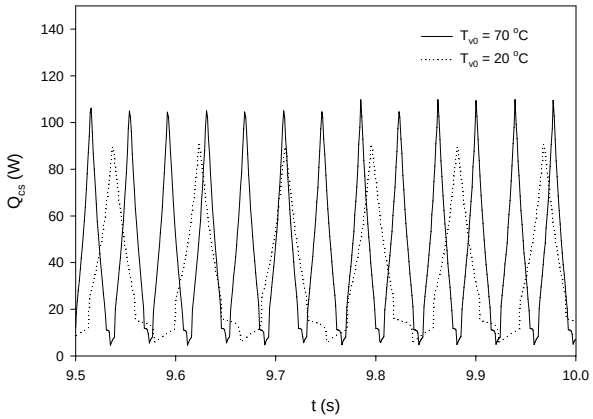

(b) Sensible heat transferred out of the liquid slug

Figure 10 sensible heat transferred for different initial temperature

Figure 9 shows the effect of the initial temperature on the latent heat transfer. It can be seen from Fig. 10(a) that the latent heat transfer into the vapor experiences a sharp increase in its magnitude is due to large rate of vapor temperature change with time when the liquid moves from left to right. Similarly, the latent heat transferred out of the vapor shown in Fig. 9 (b) experiences a decrease in its magnitude. The sensible heat transferred into and out of the system also exhibits the similar trend as above (see Figs. 10 (a) and (b)), i.e. the sensible heat transfer rate decreases with decreasing initial temperature. The system with initial temperature of 20 °C has lower average heat transfer rate of 32.29 W compared with 42.71 W for the system with an initial temperature of 70°C.

Simulations are then carried out for the cases with pressure loss at the bend and the results are compared with the case without pressure loss at the bend in Figs. 11 through 16. The radius of the bend (see Fig. 1) is 5.83 mm[16], which results in a pressure loss coefficient of $K = 0.31$. Figure 11 (a) shows the effect of the pressure loss at the bend on the oscillation of liquid slug during the first second. It can be seen that the pressure loss at the bend does not have significant effects on the amplitudes and angular frequencies of the oscillation at the first second. The effect of the pressure loss at the bend on the oscillation of liquid slug after steady oscillation is established is shown in Fig. 11(b). It can be seen that the pressure loss at the bend delays the phase of oscillation. The phase of oscillation without pressure loss at the bend is half period ahead of that for pressure loss at the bend while the frequency of oscillation is not affected by the pressure loss at bend. In addition, the pressure loss at the bend also causes very insignificant decrease of the amplitude of the liquid slug oscillation.

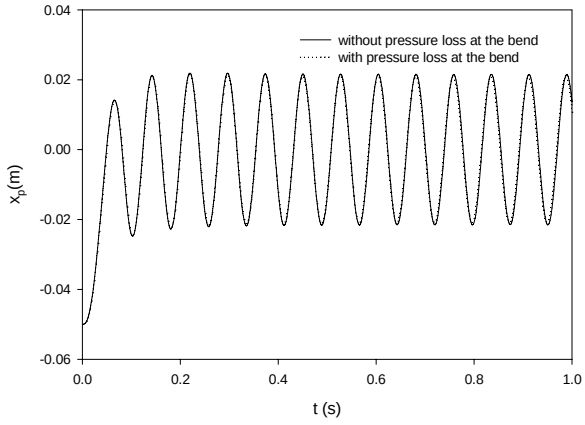

(a) Startup stage

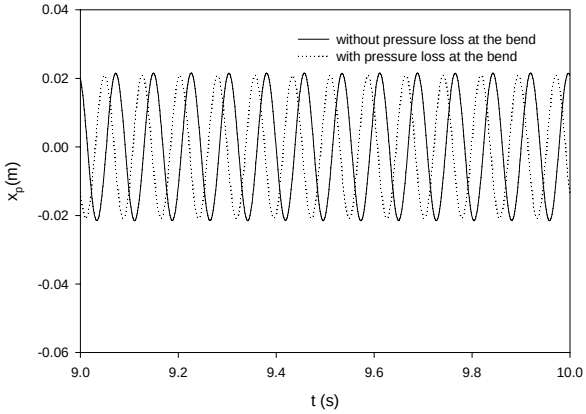

(b) Steady oscillation

Figure 11 Effect of pressure loss in bend on liquid slug displacement

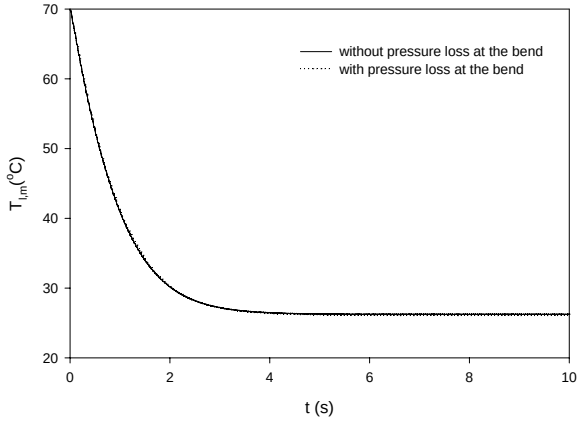

Figure 12 Effect of pressure loss in bend on the average mean temperature of liquid slug

Figure 12 shows the transient response of average mean temperature of liquid slug for the cases with and without pressure loss at the bend. It can be seen that the steady oscillations for both cases are achieved almost at the same time. Moreover, the average mean temperatures of liquid slug for the cases with and with pressure loss are almost the same. Therefore, the pressure loss at the bend has no effect on the liquid slug mean temperatures. Figures 13 and 14 show the variations of vapor temperature and pressure for the cases with and without pressure loss at the bend. Similar trend as the displacement of liquid slug can be observed from these two figures. The oscillation of vapor temperature and pressure has a half period delay with pressure loss at the bend. In addition, the pressure loss at the bend also slightly decreases the amplitudes of the oscillation of vapor temperature and pressure although the frequency remains the same.

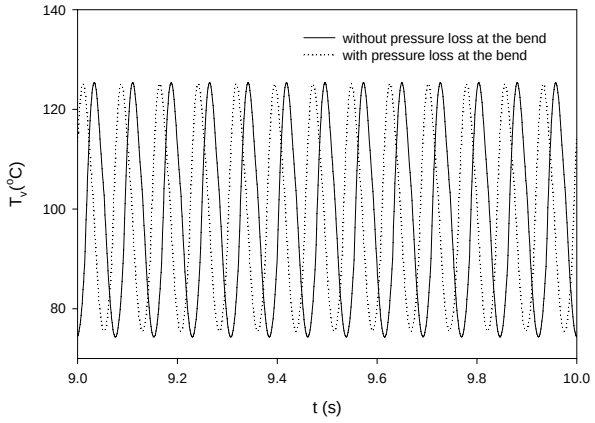

(a) Left vapor plug

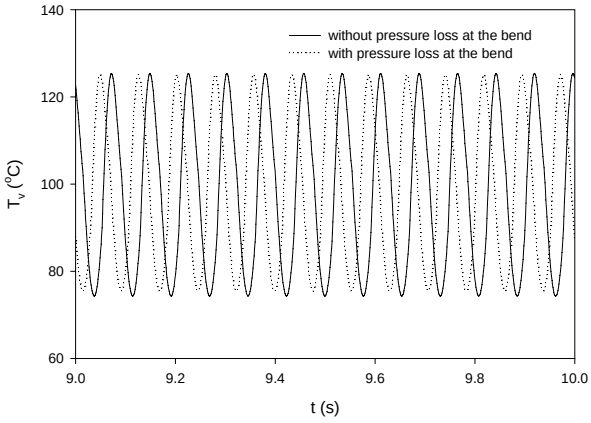

(b) Right vapor plug

Figure 13 Effect of pressure loss in bend on the vapor temperatures

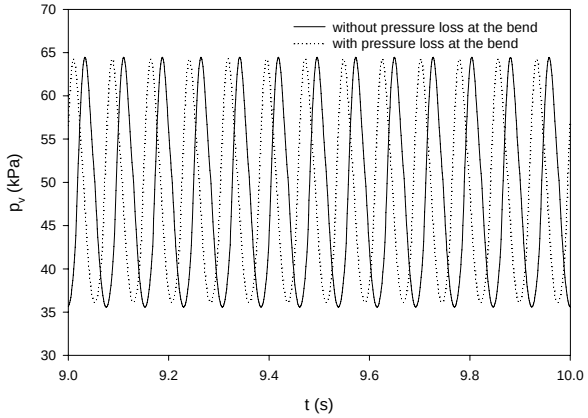

(a) Left vapor plug

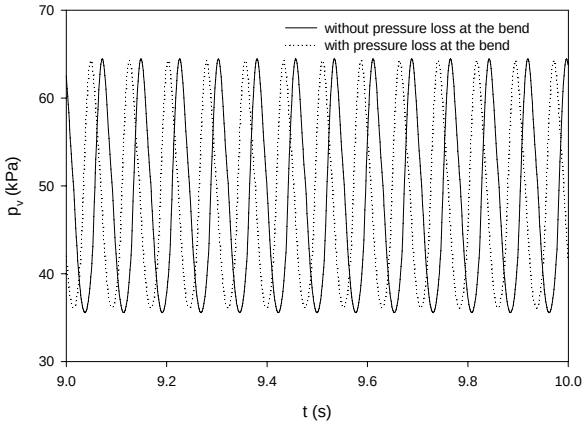

(b) Right vapor plug

Figure 14 Effect of pressure loss in bend on the vapor pressures

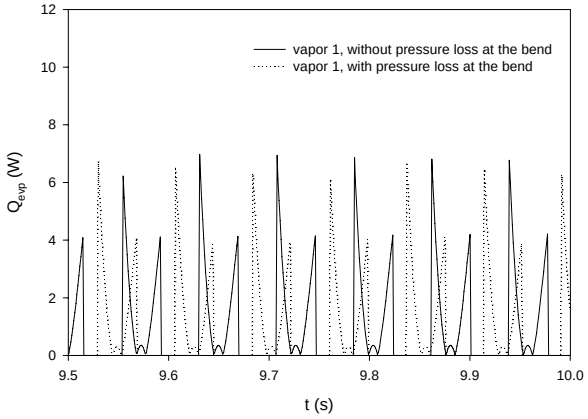

(a) Evaporation

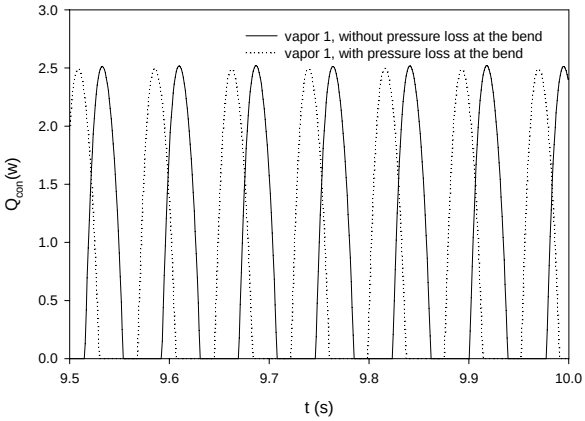

(b) Condensation

Figure 15 Effect of pressure loss in bend on evaporation and condensation of the left vapor plug

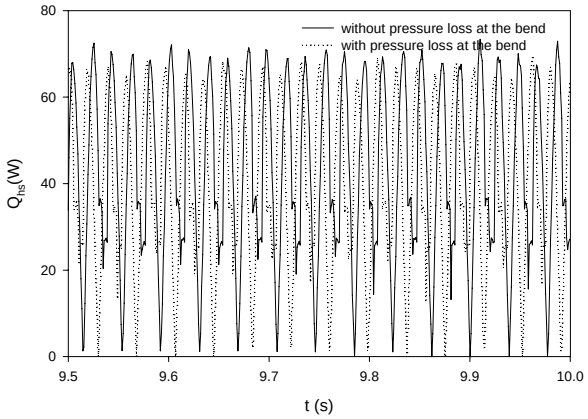

(a) Sensible heat transferred into the liquid slug

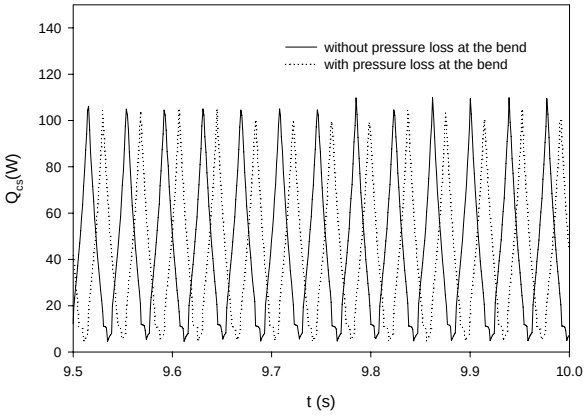

(b) Sensible heat transferred out of the liquid slug

Figure 16 Effect of pressure loss in bend on sensible heat transfer

The effect of pressure loss at bend on the latent heat transfer is shown in Fig. 15, which has a similar trend of the displacement of liquid slug oscillation. There is only a phase delay after including pressure loss at the bend and a little decrease on the amplitude of the latent heat transfer although the frequency remains the same. Figure 16 shows the effect of pressure loss at the bend on the sensible heat transferred into and out of the system. The sensible heat transfer also demonstrated the similar trend: there is only a phase delay after including pressure loss at the bend and a little decrease of the sensible heat transfer and the frequency remains unchanged. The system without pressure loss at the bend has higher average heat transfer rate than the system with pressure loss. The heat transfer performances for the cases simulated in this paper are summarized in Table 2. It can be seen that the heat transfer in an OHP is mainly due to the exchange of sensible heat, which agrees with the results obtained by Shafii et al.[11, 12].

Table 2 Total heat transport rate and contribution of latent and sensible heat transfer

Initial temperature	Nusselt Number	Pressure loss at the bend	d (mm)	T_e	$\overline{Q_{evp}}$ (W)	$\overline{Q_{h,s}}$ (W)	$\overline{Q_t}$ (W)	$\overline{Q_{h,s}}/\overline{Q_t}$ (%)
70°C	uniform	No	3.34	123.4	1.82	40.85	42.67	95.7
70°C	variable	No	3.34	123.4	1.82	42.71	44.53	95.9
20°C	variable	No	3.34	123.4	1.01	32.29	33.3	98.8
70°C	variable	No	1.67	123.4	0.83	16.91	17.74	95.3
70°C	variable	Yes	3.34	123.4	1.34	17.94	19.28	93.0

V. Conclusions

Heat transfer models in the evaporator and condenser sections of a U-shaped minichannel are developed by analyzing the effects of axial variation of surface temperature, initial temperature of working fluid, and pressure at the bend. The results confirmed that for all cases, heat transfer in an OHP is mainly due to the exchange of sensible heat. The effect of axial variation of surface temperature for laminar regime on the overall heat transfer is important. The effect of initial temperatures of working fluid on the oscillation and heat transfer is very significant. The effect of pressure loss at the bent on the momentum equation of liquid slug is studied and the results show that its effects on the flow motion and heat transfer cannot be neglected. It dampened the amplitude of the oscillation and slowed down the oscillation.

References

[1]Akachi, H., "Looped Capillary Heat Pipes," Japanese Patent, No. Hei697147, 1994

[2]Zhang, Y., and Faghri, A., "Advances and Unsolved Issues in Pulsating Heat Pipes," *Heat Transfer Engineering*, Vol.29, No. 1, 2008, pp. 20-44

[3]Lee, W.H., Jung, H.S., Kim, J.H., and Kim, J.S., "Flow Visualization of Oscillating Capillary Tube Heat Pipe," *Proceedings of the 11th International Heat Pipe Conference*, Tokyo, Japan, 1999, pp. 131-136

[4]Khandeker, S., Schneider, M., Schafer, P., Kulenovic, R., and Groll, M., "Thermo-fluid-dynamic Study of Flat Plate Closed Loop Pulsating Heat Pipes," *Microscale Thermophysical Engineering*, Vol. 6, No. 4, 2002, pp. 303-318

[5]Khandekar, S., Dollinger, N., and Groll, M., "Understanding Operational Regimes of Pulsating Heat Pipes: An Experimental Study," *Applied Thermal Engineering*, Vol. 23, No.6, 2003, pp.707-719

[6]Charoensawan, P., Khandekar S., Groll, M., and Terdtoon, P., "Closed Loop Pulsating Heat Pipes: Part A: Parametric Experimental Investigations," *Applied Thermal Engineering*, Vol. 23, 2003, pp.2009-2020.

[7]Rittidech S., Terdtoon, P., Murakami, M., Kamonpet, P., and Jompakdee, W., "Correlation to Predict Heat Transfer Characteristics of a Closed-End Oscillating Heat Pipe at Normal Operating Condition," *Applied Thermal Engineering*, Vol.23, No.4, 2003, pp. 497-510

[8]Tong, B., Wong, T., and Ooi, K., "Closed-loop Pulsating Heat Pipe," *Applied Thermal Engineering*, Vol.21, No.18, 2001, pp. 1845-1862

[9]Dobson, R.T., and Harms, T.M., "Lumped Parameter Analysis of Closed and Open Oscillatory Heat Pipe," *Proceedings of the 11th International Heat Pipe Conference*, Tokyo, Japan, 1999, pp.137-142

[10]Zhang, Y., Faghri, A., and Shafii, M.B., "Analysis of Liquid-Vapor Pulsating Flow in a U-shaped Miniature Tube," *International Journal of Heat and Mass Transfer*, Vol.45, No.18, 2002, pp.2501-2508

[11]Shafii, M.B., Faghri, A., and Zhang, Y., "Thermal Modeling of Unlooped and Looped Pulsating Heat Pipes," *ASME Journal of Heat and Mass Transfer*, Vol.123, No.6, 2001, pp.1159-1171

[12]Shafii, M.B., Faghri, A., and Zhang, Y., "Analysis of Heat transfer in Unlooped and Looped Pulsating Heat Pipes," *International Journal of Numerical Methods for Heat & Fluid Flow*, Vol.12, No.5, 2002, pp.585-609

[13]Groll, M., Khandekar, S., "Pulsating Heat Pipes: Progress and Prospects," *Proceedings of International Conference on Energy and the Environment*, Shanghai, China, Vol. 1, 2003, pp.723-730,

[14]Liang, S. B., and Ma, H. B., "Oscillating Motions of Slug Flow in Capillary Tubes," *International Communications in Heat and Mass Transfer*, Vol. 31, No.3, 2004, pp. 365-375

[15]Zhang, Y., and Faghri, A., "Oscillating Flow in Pulsating Heat Pipes with Arbitrary Numbers of Turns," *AIAA Journal of Thermophysics and Heat Transfer*, Vol.17, No.3, 2003, pp.755-764

[16]Ma, H.B., Borgmeyer, B., Cheng, P., and Zhang, Y., "Heat Transport Capability in an Oscillating Heat Pipe," *Journal of Heat transfer*, Vol. 130, 2008, pp. 081501.1-081501.7

[17]Rohsenow, W.M., Hartnett, J.P. and Ganic, E.N., *Handbook of Heat Transfer Fundamentals*, 2nd ed., McGraw-Hill, New York, 1985, Chap.7

[18]Kays, W.M., Crawford, M.E., and Weigand, B., Convective Heat Transfer, 4th ed., McGraw-Hill, New York, Chap. 8.

[19] Patankar, S.V., Numerical Heat Transfer and Fluid Flow, Hemisphere, New York, 2004, Chaps.2, 3